



Incidence and Effects of Acquisition of the Phage-Encoded *ssa* Superantigen Gene in Invasive Group A *Streptococcus*

Chuan Chiang-Ni^{1,2,3,4*}, Yen-Shan Liu², Chieh-Yu Lin², Chih-Yun Hsu¹, Yong-An Shi², Yi-Ywan M. Chen^{1,2,3}, Chih-Ho Lai^{1,2,3} and Cheng-Hsun Chiu^{2,3,5}

¹Department of Microbiology and Immunology, College of Medicine, Chang Gung University, Taoyuan, Taiwan,

²Graduate Institute of Biomedical Sciences, College of Medicine, Chang Gung University, Taoyuan, Taiwan,

³Molecular Infectious Disease Research Center, Chang Gung Memorial Hospital, Linkou, Taiwan,

⁴Department of Orthopedic Surgery, Chang Gung Memorial Hospital, Linkou, Taiwan, ⁵Division of Pediatric Infectious Diseases, Department of Pediatrics, Chang Gung Memorial Hospital, Linkou, Taiwan

OPEN ACCESS

Edited by:

Mattias Collin,
Lund University, Sweden

Reviewed by:

Aftab Jasir,
Independent Researcher,
Stockholm, Sweden
Stephen B. Beres,
Houston Methodist Research
Institute, United States

*Correspondence:

Chuan Chiang-Ni
entchuan@gap.cgu.edu.tw

Specialty section:

This article was submitted to
Infectious Diseases,
a section of the journal
Frontiers in Microbiology

Received: 25 March 2021

Accepted: 12 May 2021

Published: 04 June 2021

Citation:

Chiang-Ni C, Liu Y-S, Lin C-Y,
Hsu C-Y, Shi Y-A, Chen Y-YM,
Lai C-H and Chiu C-H (2021)
Incidence and Effects of Acquisition
of the Phage-Encoded *ssa*
Superantigen Gene in Invasive
Group A *Streptococcus*.
Front. Microbiol. 12:685343.
doi: 10.3389/fmicb.2021.685343

The acquisition of the phage-encoded superantigen *ssa* by scarlet fever-associated group A *Streptococcus* (*Streptococcus pyogenes*, GAS) is found in North Asia. Nonetheless, the impact of acquiring *ssa* by GAS in invasive infections is unclear. This study initially analyzed the prevalence of *ssa*+ GAS among isolates from sterile tissues and blood. Among 220 isolates in northern Taiwan, the prevalence of *ssa*+ isolates increased from 1.5% in 2008–2010 to 40% in 2017–2019. Spontaneous mutations in *covR/covS*, which result in the functional loss of capacity to phosphorylate CovR, are frequently recovered from GAS invasive infection cases. Consistent with this, Phostag western blot results indicated that among the invasive infection isolates studied, 10% of the *ssa*+ isolates lacked detectable phosphorylated CovR. Transcription of *ssa* is upregulated in the *covS* mutant. Furthermore, in *emm1* and *emm12 covS* mutants, *ssa* deletion significantly reduced their capacity to grow in human whole blood. Finally, this study showed that the *ssa* gene could be transferred from *emm12*-type isolates to the *emm1*-type wild-type strain and *covS* mutants through phage infection and lysogenic conversion. As the prevalence of *ssa*+ isolates increased significantly, the role of streptococcal superantigen in GAS pathogenesis, particularly in invasive *covR/covS* mutants, should be further analyzed.

Keywords: group A *Streptococcus*, streptococcal superantigen, SSA, CovR/CovS, superantigen, invasive GAS infection

INTRODUCTION

Streptococcus pyogenes [group A *Streptococcus* (GAS)] is a gram-positive bacterium that causes diseases like pharyngitis, pyoderma, scarlet fever, necrotizing fasciitis, and toxic shock syndrome. In 2011, a scarlet fever outbreak was reported in Hong Kong (Hsieh and Huang, 2011; Tse et al., 2012). The scarlet fever isolates typically harbor phage-associated superantigen genes *ssa* and *speC*, and the DNase gene *spd1* (Tse et al., 2012; Ben Zakour et al., 2015). Luk et al. (2012) found insufficient evidence to support the association between increased scarlet fever incidence or severity and a particular *emm* type, virulence gene profile, or the presence of

specific foreign genetic elements. Nonetheless, Davies et al. (2015) showed that *ssa* is absent in the clade not associated with scarlet fever, but variably present (95% isolates) in scarlet fever-associated clades, suggesting that *ssa* acquisition could be potentially related to the expansion of scarlet fever-associated *emm12*-type clones within the Hong Kong population.

An recent increased incidence of scarlet fever has also been reported in South Korea, Singapore, England, and Germany (Turner et al., 2016; Park et al., 2017; Brockmann et al., 2018; Kim and Cheong, 2018; Lamagni et al., 2018; Walker and Brouwer, 2018; You et al., 2018; Yung and Thoon, 2018). Park et al. (2017) showed that *emm4*, *emm28*, *emm1*, and *emm3* contributed to scarlet fever in South Korea. Notably, antibiotic resistance was uncommon in these scarlet fever-associated isolates (Park et al., 2017). Interestingly in England, the most prevalent isolates recovered during a national increase in scarlet fever incidence in 2016 were an emergent clone of the *emm1* MIT1 genetic lineage, designated MIT1_{UK}, which was characterized by increased production of the phage-encoded SpeA superantigen (Lynskey et al., 2019). This contrasts with the results in Hong Kong and Beijing where during an increased incidence of scarlet fever cases in 2011. The most prevalent isolates recovered were polyclonal *emm12* strains and the vast majority of which were characterized by the presence of the phage-encoded streptococcal superantigen (SSA; Davies et al., 2015). These findings show that *emm* type, antibiotic-resistant phenotype, and superantigen gene in scarlet fever-associated isolates vary from country to country; therefore, the specific factors leading to scarlet fever resurgence are not completely understood.

Streptococcal superantigen is a 260-residue protein with 60% sequence identity to that of staphylococcal enterotoxin B (SEB; Reda et al., 1994). Brouwer et al. (2020) showed that glutathione from streptolysin O (SLO)-lysed host cells not only enhances SSA production but also activates its superantigen activity. *ssa* has been detected in the toxic shock syndrome related M3 isolates (Mollick et al., 1993), suggesting it to be a potential virulence factor of GAS. As the prevalence of *ssa+* GAS isolates was >70% in certain geographic areas (Li et al., 2020a), the effects of *ssa* acquisition or *ssa+* isolate dissemination on GAS diseases need to be further clarified.

Previous studies have reported that isolates with spontaneous mutations in the *covR/covS* operon are highly related to severe diseases such as necrotizing fasciitis and toxic shock syndrome (Ikebe et al., 2010; Friaes et al., 2015). *CovR/CovS* is a two-component regulatory system in GAS, and intracellular *CovR* is phosphorylated by the sensor kinase *CovS* (Trevino et al., 2009; Tran-Winkler et al., 2011). Mutations in the *covR/covS* operon increase the production of virulence factors such as hyaluronic acid capsule, M protein, SLO, and streptokinase (Tran-Winkler et al., 2011; Chiang-Ni et al., 2017; Horstmann et al., 2018). Furthermore, *CovR/CovS* also regulates the expression of phage-related genes such as DNase *sda1* (Walker et al., 2007). Increased *Sda1* expression by a *covS* mutant promoted bacterial escape from immune clearance by degrading the DNA structure of the neutrophil extracellular traps (Walker et al., 2007).

In this study, we found that four *ssa+* isolates lacked phosphorylated *CovR*, and *ssa* transcription was upregulated in these isolates. In line with the repression in *ssa* and *slo* transcription by the *CovR/CovS* system, *ssa* deletion in the *emm1* and *emm12 covS* mutants attenuated bacterial growth activity in human blood, suggesting that *ssa* acquisition by *covS* mutants or spontaneous mutations in the *covR/covS* operon of *ssa+* isolates could enhance bacterial survival during infection. As the prevalence of *ssa+* isolates dramatically increased in northern Taiwan, the impact of the dissemination of *ssa+* isolates on our society should be continuously monitored and studied.

MATERIALS AND METHODS

Bacterial Isolates and Culture Conditions

Group A *Streptococcus* isolates from sterile tissues [ascites (2), blood (199), deep tissue (14), pleural fluid (3), and synovial fluid (2)] collected during 2008–2019 (220 isolates) at the LinKou Chang Gung Memorial Hospital (Taiwan) were included in this study. The *emm1* wild-type A20 strain, its *covR* mutant, *covS* mutant AP3, and the *CovS* kinase-inactivated (*CovS*_{H280A}) mutant were described previously (Chiang-Ni et al., 2016, 2017). GAS strains were cultured on trypticase soy agar with 5% sheep blood or in tryptic soy broth (Becton, Dickinson and Company; Sparks, MD, United States) supplemented with 0.5% yeast extract (TSBY). *Escherichia coli* DH5 α was purchased from Yeastern Biotech Co., LTD. (Taipei, Taiwan) and was cultured in Luria-Bertani (LB; Becton, Dickinson and Company; Sparks, MD, United States) broth at 37°C with vigorous aeration. When appropriate, chloramphenicol (25 μ g/ml and 3 μ g/ml for *E. coli* and GAS, respectively) and spectinomycin (100 μ g/ml) were used for selection. This study was approved by the Institutional Review Board (201900274B0 and 202000479B0) of Chang Gung Memorial Hospital, Taiwan.

Erythromycin and Clindamycin Susceptibility Test

The susceptibility of GAS isolates to erythromycin and clindamycin was determined using a disk diffusion assay according to the Clinical and Laboratory Standards Institute Guideline (Clinical and Laboratory Standards Institute, 2018). Inducible clindamycin resistance in GAS isolates was determined using the D test with erythromycin and clindamycin disks. A flattened inhibition zone around the clindamycin disk proximal to the erythromycin disk was considered a positive result.

DNA Manipulations

Genomic DNA was extracted using a previously described method (Chiang-Ni et al., 2019a), and *emm* typing, PCR amplification, and DNA sequencing were performed according to the protocol from the Centers for Disease Control and Prevention.¹ The *ssa* and erythromycin resistance genes (*mefA*,

¹<https://www.cdc.gov/streplab/groupa-strep/emm-typing-protocol.html>

ermB, and *ermTR*) were screened for by PCR amplification using previously described primers (Table 1; Meisal et al., 2010; Villasenor-Sierra et al., 2012).

Southern Blot Hybridization

Group A *Streptococcus* chromosomal DNA was digested using *Hind*III, and the DNA fragments were resolved on 0.9% agarose gel. The PCR product of the chloramphenicol cassette (716 bp; Table 1) was labeled with alkaline phosphatase as the probe, and DNA hybridization was performed according to the manufacturer's instructions (AlkPhos Direct Labeling and Detection System; GE Healthcare UK Limited; Amersham, United Kingdom). The signal was detected using a Gel Doc XR+ system (Bio-Rad; Hercules, CA, United States).

ssa and *covS* Isogenic Mutant Construction

ssa and flanking upstream and downstream regions (1805 bp) were amplified using primers *ssa*-*Bam*HI-F and *ssa*-*Bam*HI-R (Table 1), and the PCR product was ligated into a T-A cloning vector (Yeastern Biotech). *ssa* was removed by PCR with reverse primers *ssa*-*Sac*II-F and *ssa*-*Sac*II-R (Table 1) and replaced by the chloramphenicol cassette from Vector78 (Tsou et al., 2010) at the *Sac*II site. The *ssa* knockout DNA fragment was sub-cloned into the temperature-sensitive vector pCN143 (Chiang-Ni et al., 2016) at the *Bam*HI site (designed as pCN211). The plasmids pCN211 and pCN160 (Chiang-Ni et al., 2019a) were transformed into *emm*12 SPY128 and *emm*1 SPY131, respectively, by electroporation for allelic exchange, and the transformants were selected using 3 µg/ml chloramphenicol as described previously (Chiang-Ni et al., 2019b). *ssa* and *covS* deletion in the selected transformants was confirmed by Sanger sequencing. To construct *covS* and *ssa* double mutants, pCN160 was transformed into *ssa* mutants. *covS* deletion in these *ssa* mutants was selected according to the encapsulated phenotype and confirmed by Sanger sequencing.

RNA Manipulation and Quantitative PCR Analysis

RNA extraction and reverse transcription were performed as previously described (Chiang-Ni et al., 2009). The bacterial strains were cultured for 6 h (exponential phase) and 8 h (stationary phase), and total RNA was extracted for analysis. Quantitative PCR was performed in a 20 µl mixture containing 1 µl cDNA, 0.8 µl primer (10 µM), and 10 µl Sensifast Lo-ROX premixture (Bioline, Ltd.; London, United Kingdom) according to the manufacturer's instructions. Three biological replicates were performed, and *ssa* expression level was normalized to that of *gyrA* and analyzed using the threshold cycle ($\Delta\Delta C_T$) method (Roche LightCycler® 96 System; Roche Molecular Systems, Inc.; Pleasanton, CA, United States). All values from the control and experimental groups were divided by the mean value of the control samples before statistical analysis (Valcu and Valcu, 2011). Primers used to detect *ssa* (Table 1) and *gyrA* were designed using Primer3 (v.0.4.0) according to the HKU360 sequence (NCBI accession no. CP003901.1).

Phostag Western Blot Hybridization and Western Blot Analysis

Phostag western blotting was performed as previously described (Chiang-Ni et al., 2019a). Briefly, 10 µg bacterial total protein was mixed with 6× loading dye (without boiling) and separated using 10% SDS-PAGE containing 10 µM Phostag (Wako Pure Chemical Industries, Ltd.; Richmond, VA, United States) and 0.5 M MnCl₂ for 120–140 min at 100 V at 4°C. For detecting SLO, 30 µl bacterial culture supernatants were mixed with 6× protein loading dye and separated by 12% SDS-PAGE. The separated proteins were transferred onto a polyvinylidene difluoride (PVDF) membrane (Millipore; Billerica, CA, United States), which was blocked with 5% skim milk PBST buffer (PBS containing 0.2% Tween 20) at 37°C for 1 h. *CovR* was detected by the anti-*CovR* serum (Chiang-Ni et al., 2016), and SLO was detected by the anti-SLO antibody (GeneTex;

TABLE 1 | Primers used in this study.

Primer	Use	Sequence (5'-3') ^a	Reference or source
<i>ermB</i> -1	PCR	cgagtgaaaaagtactcaacc	Villasenor-Sierra et al., 2012
<i>ermB</i> -4		agtaacggtacttaattgtttac	
<i>ermTR</i> -1	PCR	atagaaattgggtcaggaagg	Villasenor-Sierra et al., 2012
<i>ermTR</i> -4		cctgtttaccatttataaacg	
<i>mefA</i> -1	PCR	agatcattaatcactagtc	Villasenor-Sierra et al., 2012
<i>mefA</i> -2		ttctctggtactaaaagtgg	
<i>ssa</i> - <i>Bam</i> HI-F	Construction	gcgggatccgtgagcaaatggccaagaat	This study
<i>ssa</i> - <i>Bam</i> HI-R		gcgggatccgtaagcggcagaatcgaaat	
<i>ssa</i> - <i>Sac</i> II-F	Construction	tcccgcggtaaaagaaataactttatg	This study
<i>ssa</i> - <i>Sac</i> II-R		tcccgcggcatttggctacctttatat	
<i>vec78_cat</i> -F- <i>sac</i> II	Construction/Southern blot	tcccgcgggatagatttatgatatag	Chiang-Ni et al., 2018
<i>vec78_cat</i> -R- <i>sac</i> II		tcccgcggattttattcagcaagtctt	
<i>ssa</i> (qPCR)-F	qPCR	cctactccagaacaattaaaca	This study
<i>ssa</i> (qPCR)-R		ggatcttacattagcccttctac	
<i>gyrA</i> -F-3	qPCR	cgctgttgactggttgg	Chiang-Ni et al., 2016
<i>gyrA</i> -R-3		ggcgtgggttagcgtattta	

^aUnderline: restriction enzyme site.

Irvine, CA, United States). The phosphorylated and nonphosphorylated CovR and SLO were visualized using a previously described method (Chiang-Ni et al., 2020).

Whole Blood Model

The growth of GAS strains in human whole blood was studied according to a previous study with modifications (Brouwer et al., 2020). Freshly drawn heparinized venous blood from healthy adults was aliquoted (360 μ l) into wells of a 24-well plate. GAS strains were grown to the exponential phase ($OD_{600} = 0.6$) in TSBY, washed, resuspended in $1 \times$ PBS buffer at $\sim 5 \times 10^5$ colony forming unit (CFU)/ml, and added to whole blood in a final volume of 400 μ l ($\sim 5 \times 10^4$ CFU/ml). After incubating for 1.5 h at 37°C, the growth of GAS strains was analyzed by plating serial dilutions on TSBY plates. Experiments were performed with blood from three different donors.

Phage Induction, Infection, and Lysogenic Conversion

Mitomycin C (0.2 μ g/ml; Sigma-Aldrich; St. Louis, MO, United States) was added to the culture of donor strain grown to the early exponential phase and incubated at 37°C for another 4 h. Culture supernatants were passed through a 0.45 μ m filter (Millipore Ireland Ltd., Co.; Cork, Ireland) to remove bacteria and large fragments, and phage particles were collected from the filtrate by ultra-centrifugation at $112,000 \times g$ for 2 h at 10°C. The recipients were grown to the logarithmic phase in the presence of 5 mM $CaCl_2$ and then co-incubated with the phage particles at 37°C for 3 h. The bacterial suspension was plated on agar plates supplemented with chloramphenicol (3 μ g/ml) and resistant convertants were collected for Southern blotting analysis.

Statistical Analysis

Statistical analysis was performed using Prism software, version 5 (GraphPad; San Diego, CA, United States). Significant differences between multiple groups were determined using the ANOVA. Post-test for ANOVA was analyzed using Tukey's honestly significant difference test. Statistical significance was set at $p < 0.05$.

RESULTS

Prevalence of *emm* Type, *ssa*+, and Erythromycin-Resistant GAS Isolates in 2008–2019

A total of 34 different *emm* types were identified among 220 isolates, among which *emm1* (37/220; 16.8%), *emm12* (32/220; 14.5%), *emm113* (20/220; 9.1%), *emm102* (16/220; 7.3%), *emm11* (14/220; 6.4%), and *emm90* (14/220; 6.4%) accounted for 60.5% total isolates. Phage-encoded *ssa* was detected by PCR. One isolate was *ssa*+ in 2008–2010 (1/65, **Figure 1A**); however, *ssa*+ isolate prevalence increased to 6.5% (3/46) in 2011–2013, 24.5% (12/49) in 2014–2016, and 40% (24/60) in 2017–2019 (**Figure 1B**). The most prevalent *emm* types of *ssa*+ isolates were *emm12* (18/40; 45%) and *emm1* (12/40; 30%).

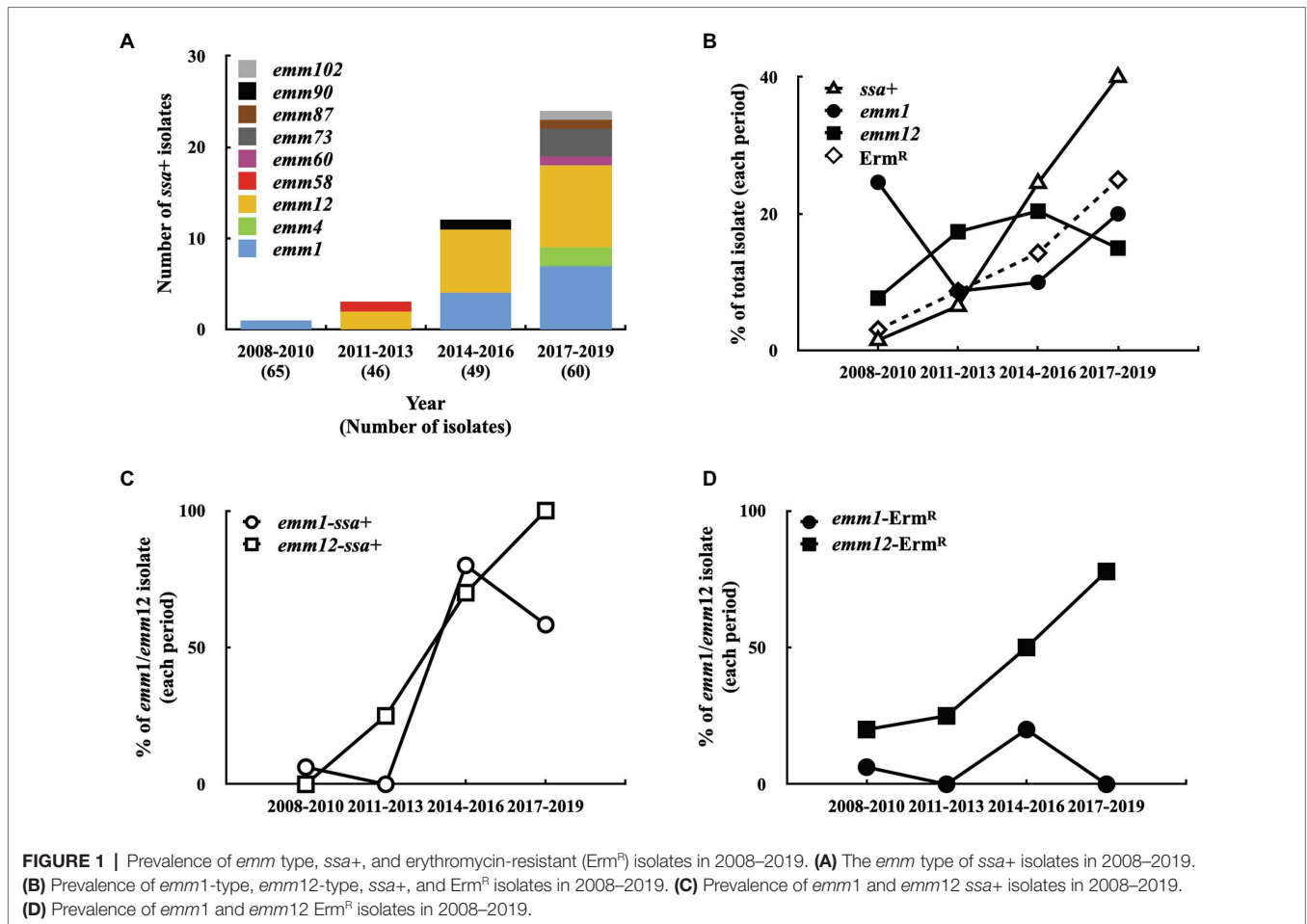
Although *emm1* and *emm12* isolate prevalence did not dramatically increase during 2008–2019 (**Figure 1B**), that of *ssa*+ *emm1* isolates increased to 58.3% (7/12) in 2017–2019 compared to 6.3% (1/16) in 2008–2010 and that of *ssa*+ *emm12* isolates increased to 100% (9/9) in 2017–2019 compared to 0% (0/5) in 2008–2010 (**Figure 1C**).

Among the 220 isolates, 28 (12.7%) were erythromycin-resistant. The prevalence of erythromycin-resistant isolates gradually increased from 3.1% (2/65) in 2008–2010 to 8.7% (4/46) in 2011–2013, 14.3% (7/49) in 2014–2016, and 25% (15/60) in 2017–2019 (**Figure 1B**). PCR analysis showed that *mefA* was detected in one erythromycin-resistant isolate (*emm12* type), and the remaining 27 erythromycin-resistant isolates were either *ermB*+ (22 isolates) or *ermTR*+ (5 isolates), indicating that these isolates were also clindamycin-resistant (**Supplementary Table S1**). In addition, 53.6% (15/28) of erythromycin-resistant isolates were type *emm12*; the prevalence of erythromycin-resistant *emm12* isolates increased from 20% (1/5) in 2008–2010 to 77.8% (7/9) in 2017–2019 (**Figure 1D**). Moreover, 77.8% (14/18) *ssa*+ *emm12* isolates were erythromycin-resistant and 92.9% (13/14) *ssa*- *emm12* isolates were erythromycin-susceptible. Although the prevalence of the *ssa*+ *emm1* isolates was increased (**Figure 1C**), only two isolates (total 37 isolates) were erythromycin-resistant. These results indicate that the prevalence of *ssa*+ isolates, particularly *emm1* and *emm12* isolates, increased. Most of the erythromycin-resistant *emm12* isolates were *ssa*+ (14/15); however, 94.6% (35/37) *ssa*+ *emm1* isolates were erythromycin-susceptible.

CovR/CovS Negatively Regulates *ssa* Transcription

Brouwer et al. (2020) showed that SSA is a thiol-activated superantigen, and its release and activity are promoted by the pore-forming toxin SLO. Moreover, the isolates from patients with invasive infection obtained spontaneous mutations in the *covR/covS* operon more frequently than those from patients with pharyngeal/tonsil infection (Ikebe et al., 2010; Friaes et al., 2015). Spontaneous inactivating mutations in *covR/covS* cause loss of CovR phosphorylation resulting in derepression of multiple secreted virulence factors including SLO (Sumby et al., 2006; Chiang-Ni et al., 2019b). In this study, after analyzing CovR phosphorylation level in 220 isolates using Phostag western blot assay, phosphorylated CovR was absent in 29 isolates (data not shown; **Supplementary Table S1**). Among the 40 *ssa*+ isolates, we identified four isolates that did not express the phosphorylated CovR protein (**Figure 2A**). Also, these four isolates expressed higher levels of SLO than those with the phosphorylated CovR protein (**Figure 2B**).

To investigate the effect of CovR phosphorylation inactivation on the *ssa* expression, isogenic *covS* mutants of *emm1*-type (SPY131) and *emm12*-type (SPY128) isolates were constructed, and *ssa* transcription was analyzed by quantitative PCR. The results showed that *ssa* expression in the *covS* mutants was 7–12-fold higher than that in the parental strains (**Figure 2C**). To further verify that *ssa* expression is repressed by phosphorylated CovR, the *covR/covS* *trans*-complementary strains of the *covS* mutants were constructed, and the phosphorylated CovR and



ssa transcription in the *covR/covS* *trans*-complementary strains were analyzed. Phostag western blot analysis showed that phosphorylated CovR was detected in the *trans*-complementary strains, but not in the vector-control strains and *covS* mutants (Figure 2D). In addition, *ssa* transcription was repressed in the *covR/covS* *trans*-complementary strains compared to that in the *covS* mutants (Figure 2D). These results indicate that *ssa* transcription is repressed by phosphorylated CovR.

The Role of SSA on *covS* Mutant Survival in Human Whole Blood

Brouwer et al. (2020) showed that the wild-type strain and *ssa* mutant had similar growth in human whole blood. *ssa* transcription and SLO production were upregulated in the *covS* mutants compared to the wild-type strains (Figures 2B,C); therefore, in this study, the role of SSA in *covS* mutant survival in human whole blood was further investigated. The *ssa* and *covS* double mutants of *emm*1-type SPY131 and *emm*12-type SPY128 were constructed. The growth of the wild-type strains, *covS*, and *ssa* mutants in the culture broth were similar (data not shown). *covS* mutants were more resistant to phagocytic killing (Sumbly et al., 2006); in agreement with this, we observed that the *covS* mutants of SPY131 and SPY128 had better growth in human blood than the wild-type strains and *ssa* mutants

(Figure 3). Furthermore, the results showed that *ssa* deletion in the *covS* mutants significantly attenuated bacterial growth in blood compared to the *covS* mutants (Figure 3), suggesting that SSA contributes to the survival of *covS* mutants in human whole blood.

Transfer of *ssa* by Phage

The *ssa*+ isolates that did not express the phosphorylated CovR protein were identified (Figure 2A). These isolates could acquire inactivating spontaneous mutations in *covR/covS* during infection. Nonetheless, the *ssa* gene is carried by phage and the possibility of *covR/covS* mutants directly acquired *ssa* by phage infection could not be excluded. Therefore, whether *covS* mutants could acquire *ssa* through phage infection and lysogenic conversion was further investigated. To select the lysogenic convertants after phage infection, *ssa* was replaced with the chloramphenicol (*cm*) cassette in the *emm*12-type SPY128 (SCN279), which was utilized as the *ssa*-encoding phage donor. After mitomycin C induction, the *cm* cassette, but not chromosomal *speB*, was detected in the filtered supernatant from SCN279 (Figure 4A), indicating that the target phage was released from SCN279. Next, the recipients, including the *emm*1-type A20 strain, its *covS* mutant AP3, and the CovS kinase-inactivated CovS_{H280A} mutant (Chiang-Ni et al., 2016, 2019b), were incubated with the collected

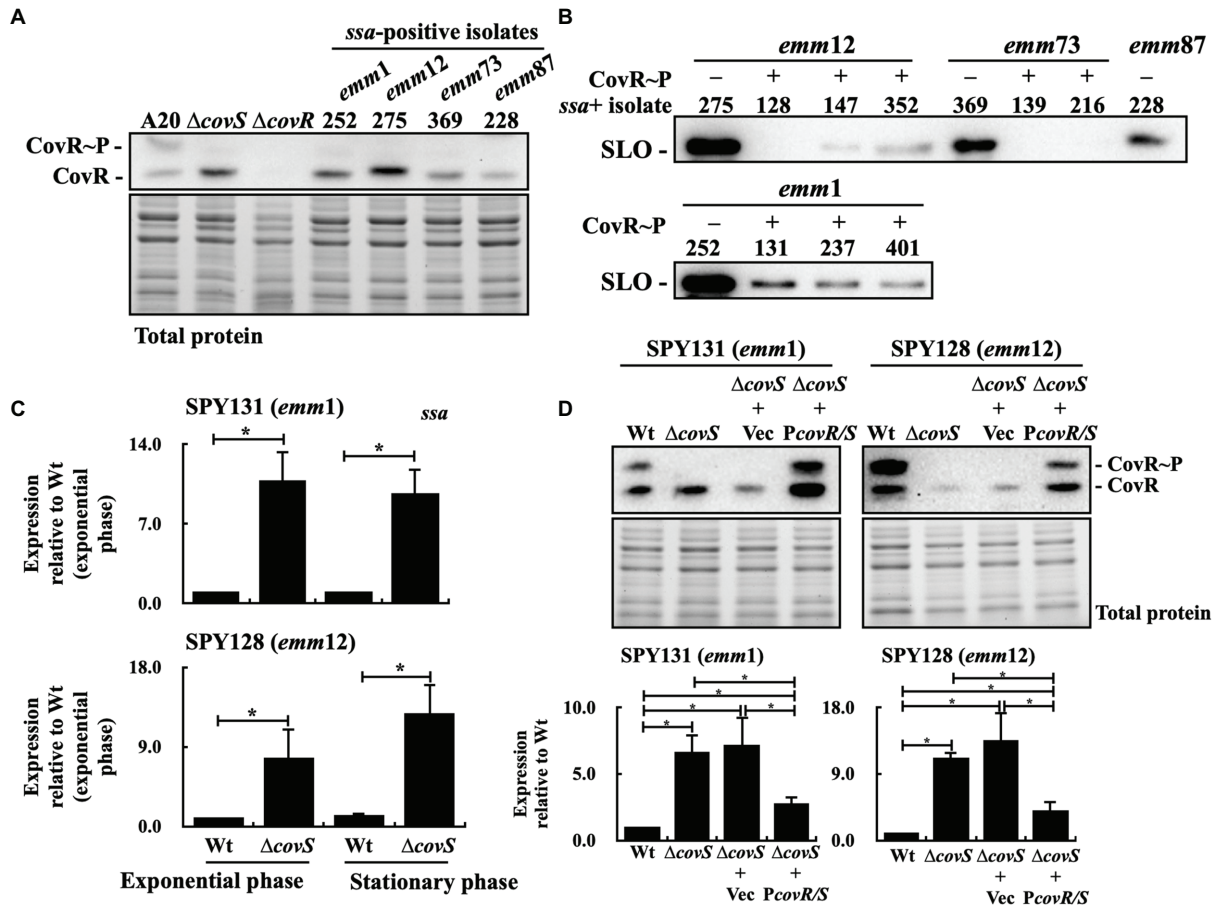


FIGURE 2 | Phosphorylated CovR and streptolysin O (SLO) expression and *ssa* transcription in selected clinical isolates, *covS* isogenic mutants, vector-control strains, and *covR/covS* trans-complementary strains. **(A)** Detection of the phosphorylated CovR in the selected clinical isolates using Phostag western blot assay. A20 and its *covS* ($\Delta covS$) and *covR* ($\Delta covR$) mutants were utilized as experimental controls. **(B)** SLO secretion in selected *ssa*-positive isolates. SLO was detected in the culture supernatants using western blot analysis. **(C)** *ssa* transcription in the SPY131 (*emm1*) and SPY128 (*emm12*; Wt) and their *covS* mutants ($\Delta covS$). **(D)** Phosphorylated CovR expression and *ssa* transcription in vector-control ($\Delta covS$ +Vec) and the *covR/covS* trans-complementary ($\Delta covS$ +PcovR/S) strains. RNA was extracted for reverse transcription-PCR (RT-qPCR) analysis. * $p < 0.05$. CovR~P, phosphorylated CovR; CovR, nonphosphorylated CovR. Total protein is served as the internal loading control.

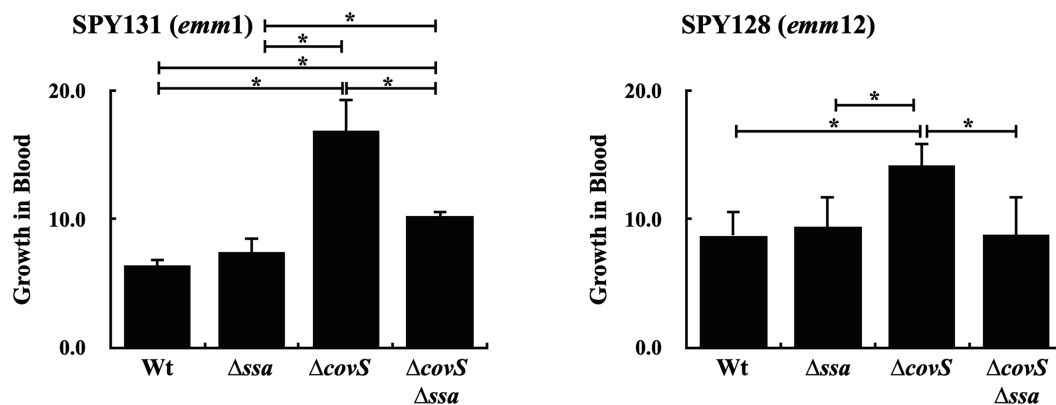


FIGURE 3 | Growth activity of SPY131 (*emm1*), SPY128 (*emm12*), their *ssa* mutants (Δssa), *covS* mutants ($\Delta covS$), and *covS* and *ssa* double mutants ($\Delta covS \Delta ssa$) in human whole blood. Group A *Streptococcus* (GAS) strains were incubated with whole blood from donors for 1.5 h. The number of surviving bacteria in human blood was determined by plating and enumerating the colony forming units (CFUs), which determined growth relative to the initial inoculum. * $p < 0.05$.

phage particles. We found that lysogenic convertants can be obtained. The *cm* cassette in the lysogenic convertants was integrated to the same insertion site of the chromosome and located on the same phage in donor strain SCN279 (Figure 4B). These results indicate that not only *emm1* wild-type strain but also its *covS* mutants could acquire *ssa* by lysogenic conversion.

DISCUSSION

This study showed that the prevalence of *ssa*+ GAS isolates increased from 1.5% (1/65) in 2008–2010 to 40% (24/60) in 2017–2019 in northern Taiwan. A total of 29 isolates could

not produce phosphorylated CovR protein, and four of these isolates were *ssa*+. We found that *ssa* transcription is repressed by phosphorylated CovR. Moreover, *ssa* gene deletion attenuated the growth activity of the *covS* mutants in human blood, suggesting that the acquisition of *ssa* by *covR/covS* mutants or spontaneous mutations in the *covR/covS* operon in the *ssa*+ isolates could be related to the increase in bacterial survival during infection.

In this study, 10% *ssa*+ isolates did not produce phosphorylated CovR under the conditions tested. Spontaneous inactivating mutations in the *covR/covS* operon increases SLO expression in GAS (Sumby et al., 2006; Chiang-Ni et al., 2019a). In addition, some clinical isolates with spontaneous mutations or

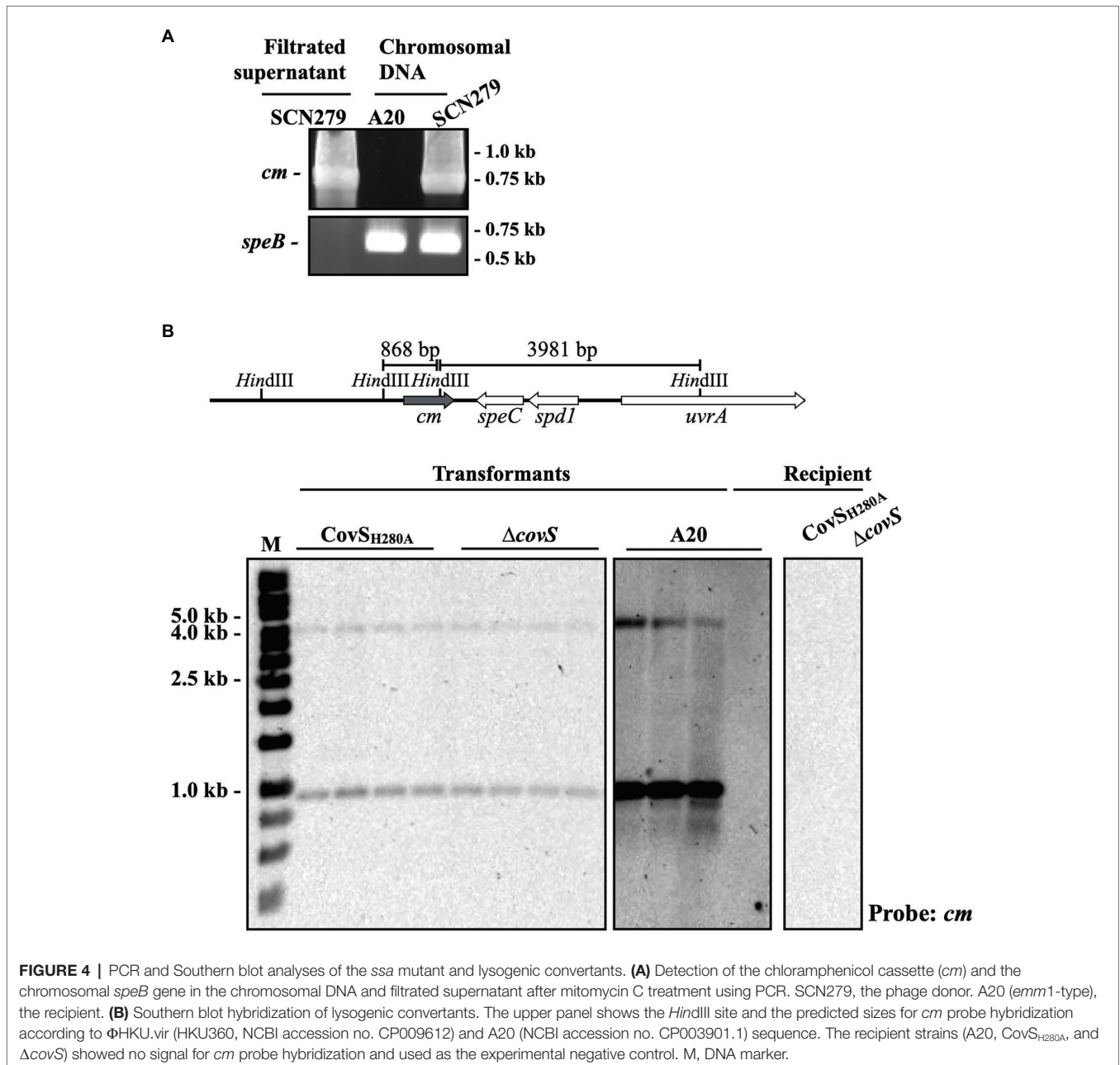


FIGURE 4 | PCR and Southern blot analyses of the *ssa* mutant and lysogenic convertants. **(A)** Detection of the chloramphenicol cassette (*cm*) and the chromosomal *speB* gene in the chromosomal DNA and filtrated supernatant after mitomycin C treatment using PCR. SCN279, the phage donor. A20 (*emm1*-type), the recipient. **(B)** Southern blot hybridization of lysogenic convertants. The upper panel shows the *HindIII* site and the predicted sizes for *cm* probe hybridization according to Φ HKU.vir (HKU360, NCBI accession no. CP009612) and A20 (NCBI accession no. CP003901.1) sequence. The recipient strains (A20, *CovS_{H280A}*, and Δ *covS*) showed no signal for *cm* probe hybridization and used as the experimental negative control. M, DNA marker.

a truncated allele of *rocA* (regulator of *cov*; upstream regulator of *CovR/CovS*) also increased the SLO expression (Feng et al., 2017; Jain et al., 2017; Horstmann et al., 2018; Chiang-Ni et al., 2020). SSA is a thio-activated superantigen, and the GAS secreted SLO, which triggers glutathione release from host cells to activate SSA *in vivo* (Brouwer et al., 2020). Brouwer et al. (2020) showed that *ssa* deletion did not attenuate bacterial survival in human blood; however, our results showed that the *covS* and *ssa* double mutants had significantly decreased growth in human blood compared to the *covS* mutants (Figure 3). As expected (Sumbly et al., 2006), the encapsulated *covS* mutant was resistant to phagocytosis (Figure 3), thus not cleared despite high expression (promoted by SLO) of the superantigen SSA, which might activate T cells and phagocytic cells. Okamoto et al. (2001) showed that macrophages in SEB-pretreated mice were less phagocytic than those in non-pretreated mice. SSA sequence is 60% identity to SEB. Based on these observations, although *covS* mutant and *covS* and *ssa* double mutant were both encapsulated, the *covS* and *ssa* double mutant might encounter higher pressure from macrophages than that of *covS* mutant. Nonetheless, these mutants were co-cultured with human whole blood for 1.5 h; whether SSA could act to macrophages like SEB during this short incubation period is not clear. Therefore, the role of SSA in GAS survival in human blood needs to be further elucidated. Whether the *ssa* transcription is directly regulated by phosphorylated *CovR* is not clear; however, our results suggest that SSA could potentially contribute to the pathogenesis of invasive *covR/covS* mutants.

Lynskey et al. (2019) showed that the toxigenic MIT1 clone (MIT1_{UK}) is related to the increased incidence of invasive GAS disease in the United Kingdom. Thereafter, the MIT1_{UK} strain was identified in Canada, the Netherlands, and the United States (Demczuk et al., 2019; Li et al., 2020b; Rumke et al., 2020), demonstrating the possibility of clonal expansion of the MIT1_{UK} clone. In Taiwan, Yan et al. (2000) showed that 64.3% erythromycin-resistant isolates were clindamycin-susceptible and harbored *mefA* before 1998. From 2001 to 2010, the erythromycin resistance rate decreased from 53.1 to 0% in southern Taiwan (Chuang et al., 2015). In this study, we found that the erythromycin resistance rate in GAS increased from 3.1% in 2008–2010 to 25% in 2017–2019. Notably, only one isolate harbored *mefA* (1/28). The changes in phenotype and genotype of erythromycin-resistant GAS suggested that the expansion of erythromycin-resistant (*ermB* and *ermTR*) and *ssa+* *emm12* clones could occur in Taiwan. In the phage infection assay, *ssa* was replaced with a chloramphenicol cassette as the selection marker, and an identical genetic element was found in the *emm12*-type donor and *emm1*-type recipient strains using Southern blot (Figure 4B and data not shown), suggesting that *ssa* could be transferred by phage. Furthermore, we also found that the chloramphenicol cassette could be transferred between *emm12*-type and *emm73*-type isolates (data not shown). These results suggest that clonal expansion and phage infection could be involved in the increased prevalence of *ssa+* isolates in Taiwan. The emerged clones in the United States (MIT1 clone) and in Asia (Hong Kong and Taiwan, *emm12* clone) are different, but both possess superantigen genes such as *speA*

and *ssa*. Nonetheless, the exact role of superantigens in the survival fitness of GAS during infection needs to be addressed.

In summary, this study showed an increased prevalence of *ssa+* and erythromycin-resistant GAS isolates in northern Taiwan, and demonstrated that *ssa* acquisition by invasive *covS* mutants or spontaneous mutations in the *covR/covS* operon of *ssa*-positive isolates could enhance bacterial growth in human blood. The role of SSA in GAS pathogenesis, particularly in invasive *covR/covS* mutants, should be further investigated.

DATA AVAILABILITY STATEMENT

The original contributions presented in the study are included in the article/Supplementary Material, further inquiries can be directed to the corresponding author.

ETHICS STATEMENT

The studies involving human participants were reviewed and approved by the Institutional Review Board (201900274B0 and 202000479B0) of the Chang Gung Memorial Hospital, Taiwan. The patients/participants provided their written informed consent to participate in this study.

AUTHOR CONTRIBUTIONS

CC-N, Y-SL, and C-YL contributed to the conceptualization, methodology, formal analysis, and writing the original draft. Y-SL, C-YL, C-YH, and Y-AS contributed to the methodology and investigation. Y-YC and C-HL contributed to the conceptualization and methodology. CC-N contributed to the writing – review and editing. CC-N and C-HC contributed to the funding acquisition. All authors contributed to the manuscript revision, read, and approved the submitted version.

FUNDING

This work was supported by parts of grants from the Chang Gung Memorial Hospital, Linkou, Taiwan (CMRPD1J0031-3 and CMRPD1K0331) and Ministry of Science and Technology, Taiwan (MOST 109-2320-B-182-036).

ACKNOWLEDGMENTS

We are grateful to the Bacterial Bank of Chang Gung Memorial Hospital, Linkou (Taiwan) for providing clinical GAS isolates.

SUPPLEMENTARY MATERIAL

The Supplementary Material for this article can be found online at: <https://www.frontiersin.org/articles/10.3389/fmicb.2021.685343/full#supplementary-material>

REFERENCES

- Ben Zakour, N. L., Davies, M. R., You, Y., Chen, J. H., Forde, B. M., Stanton-Cook, M., et al. (2015). Transfer of scarlet fever-associated elements into the group A *Streptococcus* MIT1 clone. *Sci. Rep.* 5:15877. doi: 10.1038/srep15877
- Brockmann, S. O., Eichner, L., and Eichner, M. (2018). Constantly high incidence of scarlet fever in Germany. *Lancet Infect. Dis.* 18, 499–500. doi: 10.1016/S1473-3099(18)30210-X
- Brouwer, S., Barnett, T. C., Ly, D., Kasper, K. J., De Oliveira, D. M. P., Rivera-Hernandez, T., et al. (2020). Prophage exotoxins enhance colonization fitness in epidemic scarlet fever-causing *Streptococcus pyogenes*. *Nat. Commun.* 11:5018. doi: 10.1038/s41467-020-18700-5
- Chiang-Ni, C., Chiou, H. J., Tseng, H. C., Hsu, C. Y., and Chiu, C. H. (2020). RocA regulates phosphatase activity of virulence sensor CovS of group A *Streptococcus* in growth phase- and pH-dependent manners. *mSphere* 5, e00361–e00320. doi: 10.1128/mSphere.00361-20
- Chiang-Ni, C., Chu, T. P., Wu, J. J., and Chiu, C. H. (2016). Repression of Rgg but not upregulation of LacD.1 in *emm1*-type *covS* mutant mediates the SpeB repression in group A *Streptococcus*. *Front. Microbiol.* 7:1935. doi: 10.3389/fmicb.2016.01935
- Chiang-Ni, C., Kao, C. Y., Hsu, C. Y., and Chiu, C. H. (2019a). Phosphorylation at the D53 but not T65 residue of CovR determines the repression of *rgg* and *speB* transcription in *emm1*- and *emm49*-type group A streptococci. *J. Bacteriol.* 201, e00681–e00618. doi: 10.1128/JB.00681-18
- Chiang-Ni, C., Shi, Y. A., Lai, C. H., and Chiu, C. H. (2018). Cytotoxicity and survival fitness of invasive *covS* mutant of group A *Streptococcus* in phagocytic cells. *Front. Microbiol.* 9:2592. doi: 10.3389/fmicb.2018.02592
- Chiang-Ni, C., Tseng, H. C., Hung, C. H., and Chiu, C. H. (2017). Acidic stress enhances CovR/S-dependent gene repression through activation of the *covR/S* promoter in *emm1*-type group A *Streptococcus*. *Int. J. Med. Microbiol.* 307, 329–339. doi: 10.1016/j.ijmm.2017.06.002
- Chiang-Ni, C., Tseng, H. C., Shi, Y. A., and Chiu, C. H. (2019b). Effect of phosphatase activity of the control of virulence sensor (CovS) on clindamycin-mediated streptolysin O production in group A *Streptococcus*. *Infect. Immun.* 87, e00583–e00519. doi: 10.1128/IAI.00583-19
- Chiang-Ni, C., Zheng, P. X., Ho, Y. R., Wu, H. M., Chuang, W. J., Lin, Y. S., et al. (2009). *emm1*/sequence type 28 strains of group A streptococci that express *covR* at early stationary phase are associated with increased growth and earlier SpeB secretion. *J. Clin. Microbiol.* 47, 3161–3169. doi: 10.1128/JCM.00202-09
- Chuang, P. K., Wang, S. M., Lin, H. C., Cho, Y. H., Ma, Y. J., Ho, T. S., et al. (2015). The trend of macrolide resistance and *emm* types of group A streptococci from children at a medical center in southern Taiwan. *J. Microbiol. Immunol. Infect.* 48, 160–167. doi: 10.1016/j.jmii.2013.08.015
- Clinical and Laboratory Standards Institute (2018). “Performance standards for antimicrobial susceptibility testing,” in *CLSI Supplement M100*. Wayne, PA: Clinical and Laboratory Standards Institute.
- Davies, M. R., Holden, M. T., Coupland, P., Chen, J. H., Venturini, C., Barnett, T. C., et al. (2015). Emergence of scarlet fever *Streptococcus pyogenes emm12* clones in Hong Kong is associated with toxin acquisition and multidrug resistance. *Nat. Genet.* 47, 84–87. doi: 10.1038/ng.3147
- Demczuk, W., Martin, I., Domingo, F. R., MacDonald, D., and Mulvey, M. R. (2019). Identification of *Streptococcus pyogenes* M1_{UK} clone in Canada. *Lancet Infect. Dis.* 19, 1284–1285. doi: 10.1016/S1473-3099(19)30622-X
- Feng, W., Minor, D., Liu, M., Li, J., Ishaq, S. L., Yeoman, C., et al. (2017). Null mutations of group A *Streptococcus* orphan kinase RocA: selection in mouse infection and comparison with CovS mutations in alteration of *in vitro* and *in vivo* protease SpeB expression and virulence. *Infect. Immun.* 85, e00790–e00716. doi: 10.1128/IAI.00790-16
- Friaes, A., Pato, C., Melo-Cristino, J., and Ramirez, M. (2015). Consequences of the variability of the CovRS and RopB regulators among *Streptococcus pyogenes* causing human infections. *Sci. Rep.* 5:12057. doi: 10.1038/srep12057
- Horstmann, N., Tran, C. N., Brumlow, C., DebRoy, S., Yao, H., Noguera Gonzalez, G., et al. (2018). Phosphatase activity of the control of virulence sensor kinase CovS is critical for the pathogenesis of group A *Streptococcus*. *PLoS Pathog.* 14:e1007354. doi: 10.1371/journal.ppat.1007354
- Hsieh, Y. C., and Huang, Y. C. (2011). Scarlet fever outbreak in Hong Kong, 2011. *J. Microbiol. Immunol. Infect.* 44, 409–411. doi: 10.1016/j.jmii.2011.07.003
- Ikebe, T., Ato, M., Matsumura, T., Hasegawa, H., Sata, T., Kobayashi, K., et al. (2010). Highly frequent mutations in negative regulators of multiple virulence genes in group A streptococcal toxic shock syndrome isolates. *PLoS Pathog.* 6:e1000832. doi: 10.1371/journal.ppat.1000832
- Jain, I., Miller, E. W., Danger, J. L., Pflughoeft, K. J., and Sumbly, P. (2017). RocA is an accessory protein to the virulence-regulating CovRS two-component system in group A *Streptococcus*. *Infect. Immun.* 85, e00274–e00317. doi: 10.1128/IAI.00274-17
- Kim, J. H., and Cheong, H. K. (2018). Increasing number of scarlet fever cases, South Korea, 2011–2016. *Emerg. Infect. Dis.* 24, 172–173. doi: 10.3201/eid2401.171027
- Lamagni, T., Guy, R., Chand, M., Henderson, K. L., Chalker, V., Lewis, J., et al. (2018). Resurgence of scarlet fever in England, 2014–16: a population-based surveillance study. *Lancet Infect. Dis.* 18, 180–187. doi: 10.1016/S1473-3099(17)30693-X
- Li, Y., Nanduri, S. A., Van Beneden, C. A., and Beall, B. W. (2020b). M1_{UK} lineage in invasive group A *Streptococcus* isolates from the USA. *Lancet Infect. Dis.* 20, 538–539. doi: 10.1016/S1473-3099(20)30279-6
- Li, H., Zhou, L., Zhao, Y., Ma, L., Xu, J., Liu, Y., et al. (2020a). Epidemiological analysis of group A *Streptococcus* infections in a hospital in Beijing, China. *Eur. J. Clin. Microbiol. Infect. Dis.* 39, 2361–2371. doi: 10.1007/s10096-020-03987-5
- Luk, E. Y., Lo, J. Y., Li, A. Z., Lau, M. C., Cheung, T. K., Wong, A. Y., et al. (2012). Scarlet fever epidemic, Hong Kong, 2011. *Emerg. Infect. Dis.* 18, 1658–1661. doi: 10.3201/eid1810.111900
- Lynskey, N. N., Jauneikaite, E., Li, H. K., Zhi, X., Turner, C. E., Mosavie, M., et al. (2019). Emergence of dominant toxigenic MIT1 *Streptococcus pyogenes* clone during increased scarlet fever activity in England: a population-based molecular epidemiological study. *Lancet Infect. Dis.* 19, 1209–1218. doi: 10.1016/S1473-3099(19)30446-3
- Meisal, R., Andreasson, I. K., Hoiby, E. A., Aaberge, I. S., Michaelsen, T. E., and Caugant, D. A. (2010). *Streptococcus pyogenes* isolates causing severe infections in Norway in 2006 to 2007: *emm* types, multilocus sequence types, and superantigen profiles. *J. Clin. Microbiol.* 48, 842–851. doi: 10.1128/JCM.01312-09
- Mollick, J. A., Miller, G. G., Musser, J. M., Cook, R. G., Grossman, D., and Rich, R. R. (1993). A novel superantigen isolated from pathogenic strains of *Streptococcus pyogenes* with aminoterminal homology to staphylococcal enterotoxins B and C. *J. Clin. Invest.* 92, 710–719. doi: 10.1172/JCI116641
- Okamoto, S., Kawabata, S., Nakagawa, I., and Hamada, S. (2001). Administration of superantigens protects mice from lethal *Listeria monocytogenes* infection by enhancing cytotoxic T cells. *Infect. Immun.* 69, 6633–6642. doi: 10.1128/IAI.69.11.6633-6642.2001
- Park, D. W., Kim, S. H., Park, J. W., Kim, M. J., Cho, S. J., Park, H. J., et al. (2017). Incidence and characteristics of scarlet fever, South Korea, 2008–2015. *Emerg. Infect. Dis.* 23, 658–661. doi: 10.3201/eid2304.160773
- Reda, K. B., Kapur, V., Mollick, J. A., Lamphear, J. G., Musser, J. M., and Rich, R. R. (1994). Molecular characterization and phylogenetic distribution of the streptococcal superantigen gene (*ssa*) from *Streptococcus pyogenes*. *Infect. Immun.* 62, 1867–1874. doi: 10.1128/IAI.62.5.1867-1874.1994
- Rumke, L. W., de Gier, B., Vestjens, S. M. T., van der Ende, A., van Sorge, N. M., Vlamincx, B. J. M., et al. (2020). Dominance of M1_{UK} clade among Dutch M1 *Streptococcus pyogenes*. *Lancet Infect. Dis.* 20, 539–540. doi: 10.1016/S1473-3099(20)30278-4
- Sumbly, P., Whitney, A. R., Graviss, E. A., DeLeo, F. R., and Musser, J. M. (2006). Genome-wide analysis of group A streptococci reveals a mutation that modulates global phenotype and disease specificity. *PLoS Pathog.* 2:e5. doi: 10.1371/journal.ppat.0020005
- Tran-Winkler, H. J., Love, J. F., Gryllos, I., and Wessels, M. R. (2011). Signal transduction through CsrRS confers an invasive phenotype in group A *Streptococcus*. *PLoS Pathog.* 7:e1002361. doi: 10.1371/journal.ppat.1002361
- Trevino, J., Perez, N., Ramirez-Pena, E., Liu, Z., Shelburne, S. A., Musser, J. M., et al. (2009). CovS simultaneously activates and inhibits the CovR-mediated repression of distinct subsets of group A *Streptococcus* virulence factor-encoding genes. *Infect. Immun.* 77, 3141–3149. doi: 10.1128/IAI.01560-08
- Tse, H., Bao, J. Y., Davies, M. R., Maamary, P., Tsoi, H. W., Tong, A. H., et al. (2012). Molecular characterization of the 2011 Hong Kong scarlet fever outbreak. *J. Infect. Dis.* 206, 341–351. doi: 10.1093/infdis/jis362
- Tsou, C. C., Chiang-Ni, C., Lin, Y. S., Chuang, W. J., Lin, M. T., Liu, C. C., et al. (2010). Oxidative stress and metal ions regulate a ferritin-like gene,

- dpr, in *Streptococcus pyogenes*. *Int. J. Med. Microbiol.* 300, 259–264. doi: 10.1016/j.ijmm.2009.09.002
- Turner, C. E., Pyzio, M., Song, B., Lamagni, T., Meltzer, M., Chow, J. Y., et al. (2016). Scarlet fever upsurge in England and molecular-genetic analysis in North-West London, 2014. *Emerg. Infect. Dis.* 22, 1075–1078. doi: 10.3201/eid2206.151726
- Valcu, M., and Valcu, C. M. (2011). Data transformation practices in biomedical sciences. *Nat. Methods* 8, 104–105. doi: 10.1038/nmeth0211-104
- Villasenor-Sierra, A., Katahira, E., Jaramillo-Valdivia, A. N., Barajas-Garcia Mde, L., Bryant, A., Morfin-Otero, R., et al. (2012). Phenotypes and genotypes of erythromycin-resistant *Streptococcus pyogenes* strains isolated from invasive and non-invasive infections from Mexico and the USA during 1999–2010. *Int. J. Infect. Dis.* 16, e178–e181. doi: 10.1016/j.ijid.2011.11.005
- Walker, M. J., and Brouwer, S. (2018). Scarlet fever makes a comeback. *Lancet Infect. Dis.* 18, 128–129. doi: 10.1016/S1473-3099(17)30694-1
- Walker, M. J., Hollands, A., Sanderson-Smith, M. L., Cole, J. N., Kirk, J. K., Henningham, A., et al. (2007). DNase Sda1 provides selection pressure for a switch to invasive group A streptococcal infection. *Nat. Med.* 13, 981–985. doi: 10.1038/nm1612
- Yan, J. J., Wu, H. M., Huang, A. H., Fu, H. M., Lee, C. T., and Wu, J. J. (2000). Prevalence of polyclonal *mefA*-containing isolates among erythromycin-resistant group A streptococci in southern Taiwan. *J. Clin. Microbiol.* 38, 2475–2479. doi: 10.1128/JCM.38.7.2475-2479.2000
- You, Y., Davies, M. R., Protani, M., McIntyre, L., Walker, M. J., and Zhang, J. (2018). Scarlet fever epidemic in China caused by *Streptococcus pyogenes* serotype M12: epidemiologic and molecular analysis. *EBioMedicine* 28, 128–135. doi: 10.1016/j.ebiom.2018.01.010
- Yung, C. F., and Thoon, K. C. (2018). A 12 year outbreak of scarlet fever in Singapore. *Lancet Infect. Dis.* 18:942. doi: 10.1016/S1473-3099(18)30464-X

Conflict of Interest: The authors declare that the research was conducted in the absence of any commercial or financial relationships that could be construed as a potential conflict of interest.

Copyright © 2021 Chiang-Ni, Liu, Lin, Hsu, Shi, Chen, Lai and Chiu. This is an open-access article distributed under the terms of the Creative Commons Attribution License (CC BY). The use, distribution or reproduction in other forums is permitted, provided the original author(s) and the copyright owner(s) are credited and that the original publication in this journal is cited, in accordance with accepted academic practice. No use, distribution or reproduction is permitted which does not comply with these terms.